Polaron Formation and Hopping Conduction in Hyperbranched Polymers: A Theoretical Approach

Thorsten Koslowski,*,† Aurel Jurjiu,‡ and Alexander Blumen‡

Institut für Physikalische Chemie II and Theoretische Polymerphysik, Universität Freiburg, D-79104 Freiburg im Breisgau, Germany

Received: October 29, 2003

In this work, we address the formation of polarons in hyperbranched polymers and their conduction properties from a theoretical and numerical perspective. As a chemical realization, we consider condensed triarylamine molecules. The topology of the macromolecules follows the concept of regular hyperbranched fractals. The electronic structure is described by a π orbital tight-binding Hamiltonian extended by a reaction field, which takes dielectric polarization effects into account. Excess charges are predominantly localized at the nitrogen atoms; the trapping energies and the hopping rates depend on the local environment of the monomers via their coordination numbers. For systems containing up to 64 monomers, the structures studied here provide fast charge transport along the backbone of the polymer, whereas the side chains are rapidly depopulated. We therefore suggest the use of hyperbranched triarylamines as bridging elements to enhance the mobility of holes in conducting polymers.

1. Introduction

The past decade has seen a considerable growth of interest in hyperbranched macromolecular systems.[1−8] From a topological perpective, these objects are trees, since they lack loops. Paradigmatic for this class of molecules are the dendrimers.[2−8] Being topologically equivalent to finite Cayley trees, they are constructed from a core with f branches (f denotes the coordination number), to which $f - 1$ new branches are attached in the next stage of a recursive construction. Due to the exponential increase in the number of branches at each generation, the chemical synthesis usually terminates after five or six recursive steps. Thus, in many ways these objects are atypical for polymers: they are limited in their growth and they do not obey scaling.[2−8] General tree-like structures (or hyperbranched polymers), on the other hand, are often synthesized in batch reactions,[9,10] and may scale.[11] A particular class of hyperbranched polymers are the so-called regular hyperbranched fractals (RHFs), which are a generalization of the Vicsek fractal;[12−18] the RHFs obey an iterative construction that will be detailed below. Many dynamical properties of polymers—such as the vibrational spectrum, the relaxation modes, the linear dielectric properties, and random walk aspects—depend on the eigenvalues of the corresponding connectivity matrix; for RHFs of arbitrary size these eigenvalues can be obtained analytically.[18,19]

Recently, we have advocated in favor of the synthesis of model compounds for this class of systems and suggested condensed triarylamines as a possible realization,[20] as both the corresponding bridged molecules[21] and bulk polymer phases[22] exist. Interestingly, bridged triarylamine cations exhibit mixed valency and charge transfer, features that have been studied in detail both experimentally[21] and theoretically.[23,24] As charge localization and electron transfer play an important role in chemistry, physics, and materials science,[25−31] we have studied these issues for a regular hyperbranched polymer from a theoretical perspective, using a recently suggested variational approach to the energetics of electron-transfer reactions.[23,32] From the point of view of potential applications, conducting oligomers such as oligo-*p*-phenylene or oligopyrrole may experience an enhanced conductivity once covalently bound to and cross-linked by hyperbranched polymers that enable charge transfer.

This work is organized as follows: In the next section, we describe the model underlying the topology and the microscopic structure of our system. Then we motivate and describe the Hamiltonian, which we apply in our approach. Results for the density of states and the transport properties are reported in the fourth section, and we summarize our conclusions in the final part of the paper.

2. Topology and Microscopic Structure

The general topology of RHFs is exemplified in Figure 1, which shows schematically a RHF characterized by the coordination number $f = 3$. To construct this object, one starts at generation $g = 1$ from an object of $f + 1 = 4$ sites, which are arranged in a starwise pattern, with the central bead connected to three neighbors (see the open circles in the figure). To this object, f copies are attached via f bonds in the next generation, $g = 2$, leading to a structure consisting of 16 sites. A subsequent iteration of the process leads, in an obvious way, to the $f = 3$ RHF at generation $g = 2$, shown in Figure 1. For large structures, the fractal dimension of an RHF in solution is given by[19]

$$\bar{d}_f = \frac{2\ln(f+1)}{\ln 3} \tag{2.1}$$

which leads to $\bar{d}_f \simeq 2.52$ for $f = 3$.

* Corresponding author. E-mail: thorsten.koslowski@physchem.uni-freiburg.de. Fax: (+49)761-203-6189.

† Institut für Physikalische Chemie II.

‡ Theoretische Polymerphysik.

10.1021/jp037263a CCC: $27.50
Published on Web 02/13/2004

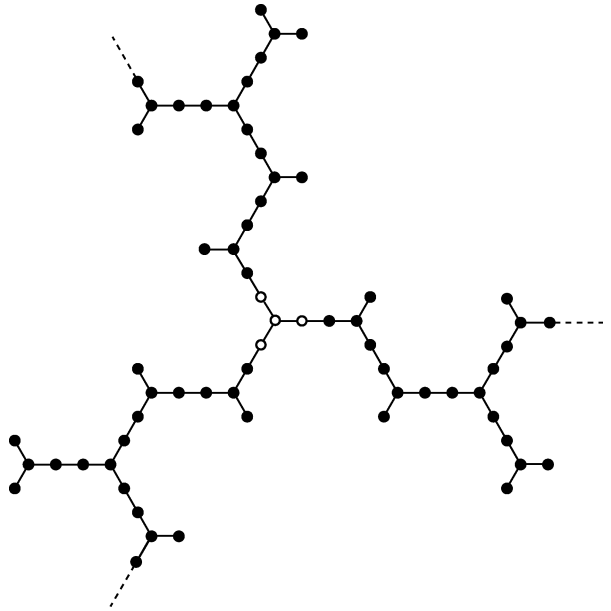

Figure 1. Vicsek fractal with connectivity $f = 3$ at generation $g = 2$. The open circles refer to the initial stage of the construction.

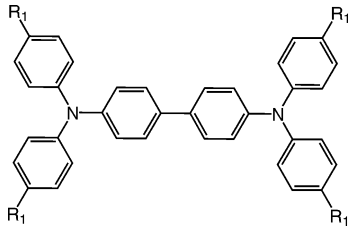

Figure 2. A bridged triarylamine molecule, R_1 = methoxy. Modeled after the work of Lambert and Nöll.[21]

Recently, we have suggested a chemical realization of this fractal in terms of the structure, steric requirements, and the synthesis of a model compound.[20] As is evident from Figure 1, RHFs are build from structural entities with valence *c*, where *c* equals 1, 2, or *f*. We denote the corresponding building blocks by M_1, M_2, and M_f, respectively. Note that the case $f = 2$ is particular, as only M_1 and M_2 appear and the linear chain is recovered. M_1, M_2, and M_f may be chosen from different chemical species, as the synthesis of hyperbranched polycarbosilanes and copolyesters has shown.[33,34] For $f = 3$, we have suggested condensed triarylamines as interesting candidates, which have been synthesized as bridged molecules (an example is depicted in Figure 2) and which exist in a polymer phase. As structural units, we use nitrogen atoms (M_3) and phenyl rings (M_1, M_2); for M_2, these are connected in the para position.

A representation of a hyperbranched triarylamine is given in Figure 3 for a RHF of generation $g = 2$. For these systems, we have a fractal dimension considerably smaller than the embedding Euclidian dimension, $d = 3$. Thus, packing problems or overcrowding, which arise at higher generations for dendrimers or for hyperbranched molecules with large *f*, do not play a role here. To verify that our RHFs are indeed well-embedded in the three-dimensional Euclidian space, we have constructed models for the generations $g = 1$, 2, and 3 and have relaxed them using a classical force field.[35] In Figure 3, a gradient-optimized structure is shown for $g = 2$. It is evident that the spatial requirements can be met; this statement also holds for force fields that lead to slightly twisted biphenyl bridges.

3. Electronic Structure

To describe the electronic structure of bridged triarylamine molecules and of polymers starting from the monomers involved, we take the bridges as planar and assume the approximate separability of the Hamiltonian into a σ and a π electron problem; here we are interested in the π states which form the frontier molecular orbitals. In the simplest approximation, the π states can be treated on the tight-binding or Hückel level. We consider the following Hamiltonian:[23]

$$\hat{H} = \sum_i \epsilon_i n_i + \sum_{i \neq j} a_i^{\dagger} a_j V_{ij} - \sum_i U_i (n_i - \bar{n}_{i,0})^2 \qquad (3.1)$$

We have creation/annihilation operators $a_i^{\dagger}/a_j$ acting upon the $2p_z$ orbitals of the nitrogen or of the carbon atoms, corresponding number operators n_i, and a reference charge of each atom within the neutral molecule, $\bar{n}_{i,0}$. The ϵ_i denote the carbon and nitrogen 2p valence ionization potentials; their difference is set to $\epsilon_C - \epsilon_N = 2.05$ eV.[23] For the hopping matrix elements, a standard parametrization scheme with $V_{ij}(r) = V_{ij}^0 \, r_0^2/r^2$ stemming from solid state theory has been used.[36] The twist of phenyl rings out of the plane defined by the bridge has been accounted for by weighting the off-diagonal tight-binding matrix elements accordingly. We take the long-range Coulomb interactions as being incorporated into effective tight-binding parameters.

The third term in eq 3.1 can be interpreted as a nonretarded reaction field, which extends the familiar LCAO approach to systems embedded in a polarizable environment.[23,32] In a straightforward extension of Marcus' treatment of the energetics of outer-sphere reactions[37] to many-site systems, we write the reorganization energy emerging from an ensemble of excess charges Δz_i localized within spheres of radii σ_i as

$$\lambda_{out} = -\frac{e^2}{4\pi\epsilon_0}\left(\frac{1}{\epsilon_\infty} - \frac{1}{\epsilon_s}\right)\left(\sum_i \frac{\Delta z_i^2}{\sigma_i} - \sum_{i<j} \frac{\Delta z_i \Delta z_j}{r_{ij}}\right) \qquad (3.2)$$

If the high- and the low-frequency dielectric response characterized by the constants ϵ_∞ and ϵ_s can be separated, this model turns into the familiar attractive Hubbard Hamiltonian[38] by replacing the charges Δz_i by the corresponding number operators $n_i - \bar{n}_{i,0}$. Neglecting the long-range Coulomb interactions, we arrive at the last term of eq 3.1. For an efficient numerical solution suitable to the large systems studied here, we apply the restricted Hartree−Fock mean field approximation[23]

$$(n_i - \bar{n}_{i,0})^2 \simeq 2n_i(\bar{n}_i - \bar{n}_{i,0}) - \bar{n}_i^2 + \bar{n}_{i,0}^2 \qquad (3.3)$$

where the overbars denote the expectation values within an iterative self-consistent-field approach; we compute these from the results of a previous step. Further details of the description of the electronic structure, the parametrization of the tight-binding Hamiltonian, and a discussion of the validity of the nonretarded approximation are provided in ref 23.

Once the nonretarded reaction field is sufficiently strong, excess charges may predominantly localize on either of the nitrogen atoms. For small molecules, the energy of the system can be computed as a function of all relevant density matrix elements (or charge orders) $\bar{n}_i$, leading to the potential energy surface of the charge-transfer reaction.[23,32] For the large systems studied here, this approach is not feasible, and we apply the linear synchronous transit approximation, as advocated by Clark for electron-transfer reactions.[39] For a singly charged cation, we compute all possible basins of attraction for the SCF

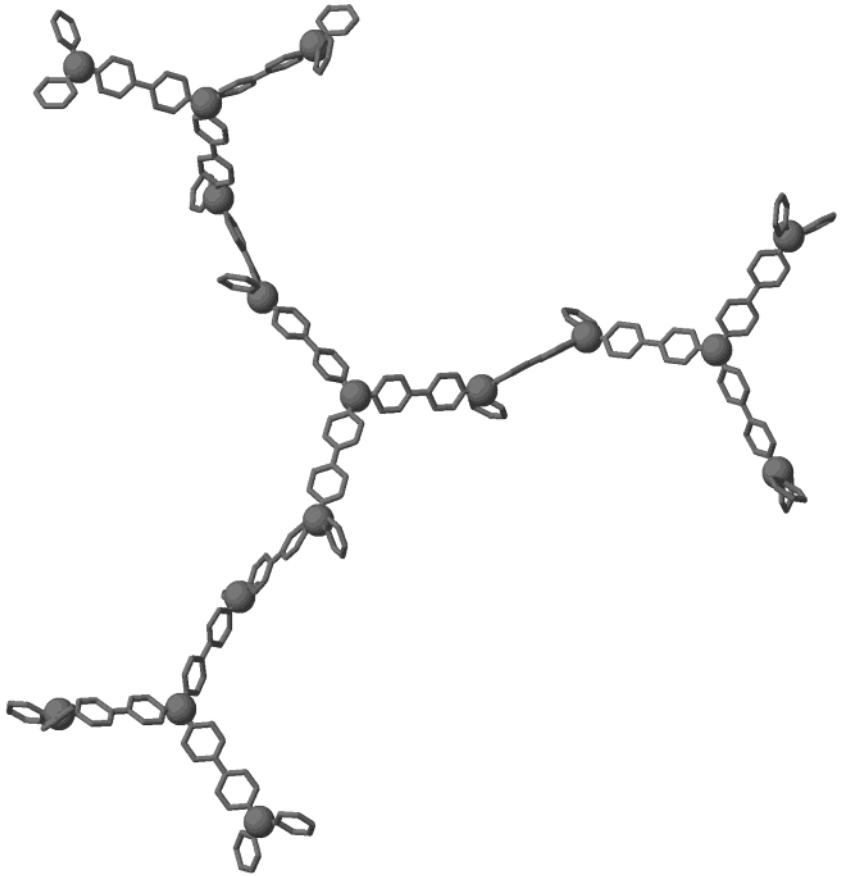

Figure 3. A chemical realization of the $f = 3$, $g = 2$ regular hyperbranched fractal obtained by replacing the monomers by triarylamine units. Shown is a gradient-optimized structure with use of a classical force field. The nitrogen atoms are indicated as large gray spheres, while the hydrogen atoms have been omitted for convenience.

procedure. Their number is given by the number of monomers (or nitrogen atoms) in the system. For two adjacent minima *A* and *B* we calculated the diagonal of the corresponding density matrices, $\{\bar{n}_{A,1}...\bar{n}_{A,N}\}$ and $\{\bar{n}_{B,1}...\bar{n}_{B,N}\}$, where the second index refers to the atomic orbitals that form the localized AO basis. We then scan the potential energy surface along the cross-section given by $\bar{n}_{i,\mathrm{int}} = \alpha\bar{n}_{i,A} + (1 - \alpha)\bar{n}_{i,B}$, where the linear interpolation parameter α serves as a reaction coordinate. In this scan, α varies between zero and unity. We now consider conduction paths connecting a series of such minima. Then the transfer can be visualized as a series of consecutive hops between neighboring minima, in which α increases by one at each elementary transfer step. We call this scheme the linear synchronous transit (LST) approach.

4. Charge Localization and Transport

In this section, we first reconsider charge transfer in the molecule from which the hyperbranched polymer is constructed (see Figure 2), and compare the parameters characteristic for charge transfer to those of a previous numerical study[23] and to experimental results.

First, we verify that the LST approach, as described above, corresponds in our molecular system to a complete scan. Here such a complete scan of the relevant elements of the electronic density matrix is feasible: the total energy can be expressed as a function of the two nitrogen charge orders. The complete scan leads to an activation barrier of 0.090 eV (as compared to the LST value of 0.093 eV) and to a low-energy cutoff of the intervalence charge-transfer spectrum at 0.419 eV, which is almost identical with its LST counterpart, namely to 0.420 eV.

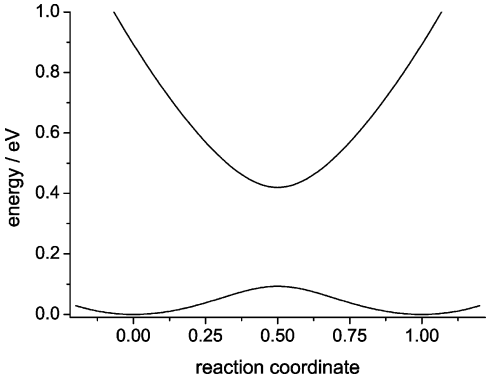

Figure 4. Ground-state and excited-state potential energy of charge transfer in the bridged triarylamine molecule (Figure 2), displayed along the minimum energy path of the reaction. See text for details.

At the transition state, the nitrogen charge orders differ only slightly; we obtain $\bar{n}_N = 1.44$ from the scan and $\bar{n}_N = 1.40$ from the LST approach.

By definition, the following holds: for the minima of the potential energy curve, the ground-state energy of the scanning procedure and the ground-state energy of the LST approach are identical, and optical excitations at these minima from the ground state to the first excited state require the same transition energy within the LST and the scanning approach. In Figure 4 we display the potential energy for charge transfer as a function of the reaction coordinate.

We now turn to the electronic structure of the chemical realization of the RHFs. For the triarylamine oligomers, an excess positive charge may localize on one of the nitrogen atoms and its close neighborhood. The basin of attraction of the SCF

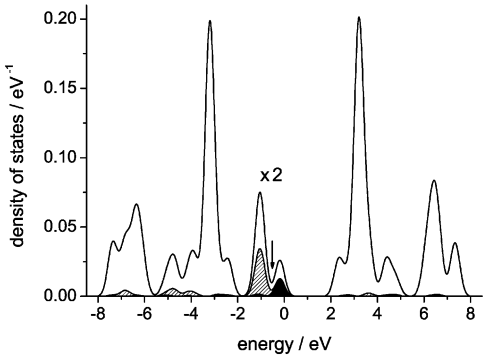

Figure 5. Electronic density of states for a regular hyperbranched fracal constructed from triarylamine molecules ($g = 1$). Shading indicates the partial density of states contributions stemming from the nitrogen atoms; the polaronic nitrogen contributions are drawn in black. The Fermi level is indicated by an arrow; the density of states has been scaled by a factor of 2 for energies between −1.8 and 1.5 eV for all curves.

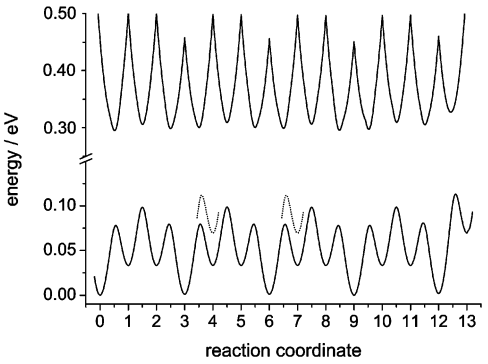

Figure 6. Energy profile for charge transport along the backbone of one arm of a triarylamine oligomer at generation $g = 3$. The dotted lines correspond to dead ends of the fractal. The upper curve displays the energy of the first excited state. For further details, see text.

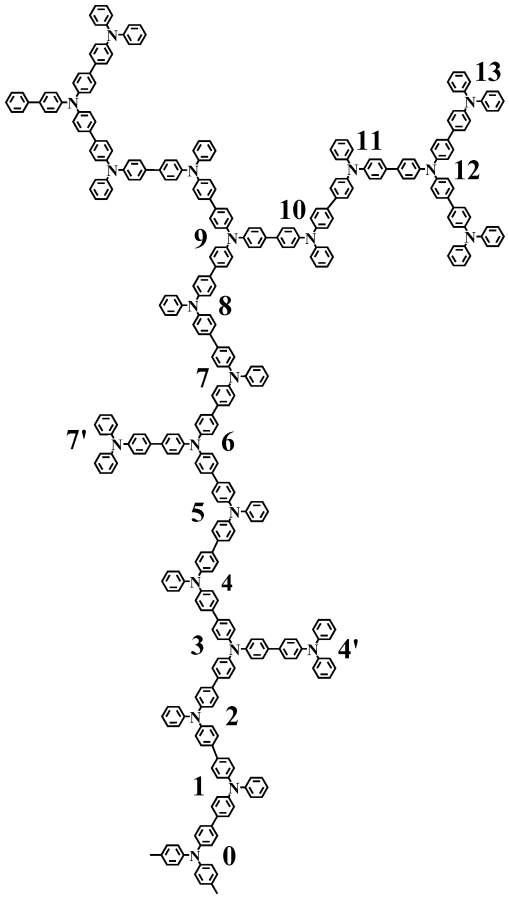

Figure 7. An arm of a triarylamine oligomer at generation $g = 3$. The integers indicate the enumeration of the polaron positions in Figure 6.

procedure that solves the electronic structure problem self-consistently, eqs 3.1 and 3.3, is determined by the initial conditions. We have studied RHFs of generations $g = 1$, 2, and 3, which give rise to systems containing 4, 16, and 64 monomers, respectively. The number of nonhydrogen atoms in the largest system then equals 1216.

For a RHF characterized by $g = 1$ we depict in Figure 5 the total DOS, the partial density of states with respect to all nitrogens (shaded) and to the particular nitrogen atom on which the polaron is localized. All curves are calculated from the discrete eigenvalues by broadening them with a Gaussian function with an RMS value of 0.2 eV. The partial DOS (PDOS) is computed by weighting the eigenstates E_a by the molecular orbital expansion coefficients c_{ia}, where i refers to the site and a to the index of the molecular orbital. The PDOS emerging from the eigenstate a is given by

$$\mathrm{PDOS}(E_a) = \sum_i{}' c_{ia}{}^2 \mathrm{DOS}(E_a) \qquad (4.1)$$

where the prime indicates the restriction of the sum over i to the atomic orbitals of interest. In Figure 5, we note that the band around the Fermi level is split into an occupied and a vacant part; the ratio of the integrals equals $1/(n-1)$, where n denotes the number of monomers. Both subbands around E_F are dominated by nitrogen contributions; the vacant part originates from a state split from the bulk of the nitrogen band due to the formation of a polaron state. Similar to the theory of inorganic polymers,[40] the oxidation of hyperbranched triarylamines thus leads to the formation of impurity bands in the one-electron density of states. For singly oxidized cations, with increasing g only the relative weight of the polaron state changes with respect to the bulk of the density of states.

In Figure 6, we display the potential energy surface obtained within the Hartree−Fock and the LST approach presented above for a RHF at generation $g = 3$, which consists of 64 condensed triarylamine units (i.e. 1216 nonhydrogen atoms). We use the underlying 3-fold symmetry of the topology, cf. Figure 3, and display only the energy landscape for hopping along one of the three branches. In what the reaction coordinate r is concerned, we start from the center of the fractal ($r = 0$) and follow a hopping path toward the periphery. We note that the sites with $r = 3k$ (k integer) have the connectivity $c = 3$ and that the connectivity of the last site equals $c = 1$. The dotted curves diplayed in Figure 6 denote paths leading to dead ends. For a better visualization of the paths considered here, we also present them in Figure 7 based on the structure formula.

As is evident from Figure 6, the energies of positive charges trapped in local basins of attraction depend mainly on the connectivity of the respective sites. Measuring the energies relative to the energy of a M_3 building block ($c = 3$), we obtain $E_2 - E_3 = +33.3$ meV and $E_1 - E_3 = +69.6$ meV. Consequently, the corresponding populations P_c increase with increasing connectivity, and we obtain $P_2/P_3 = 0.27$ and $P_1/P_3 = 0.06$ at room temperature ($T = 293$ K); these ratios decrease to $P_2/P_3 = 6.6 \times 10^{-3}$ and $P_1/P_3 = 2.8 \times 10^{-5}$ at the boiling point of liquid nitrogen ($T = 77$ K). We find as activation barriers for hopping $E_{A,3\to2} = E_{A,32} = 78.0$ meV, $E_{A,23} = 44.7$ meV, $E_{A,13} = 113.0$ meV, $E_{A,31} = 43.4$ meV, and $E_{A,22} = 65.4$

meV. These numbers have to be compared to $E_{A,11} = 90.0$ meV, the computed hopping barrier for charge transfer within the molecule displayed in Figure 2. The corresponding hopping rates can now be evaluated from

$$k_{ij} = k_0 \exp(-E_{A,ij}/k_B T) \quad (4.2)$$

with an empirical $k_0 = 9 \times 10^{12}$ s^{-1}.[21] At room temperature, we obtain from eq 4.2. the rates $k_{32} = 4.1 \times 10^{11}$ s^{-1}, $k_{23} = 1.5 \times 10^{12}$ s^{-1}, $k_{31} = 1.0 \times 10^{11}$ s^{-1}, $k_{13} = 1.6 \times 10^{12}$ s^{-1}, and $k_{22} = 6.7 \times 10^{11}$ s^{-1}. These values should be compared to the room temperature charge-transfer rate obtained for the molecule from $E_{A,11}$, which equals $k_{11} = 2.5 \times 10^{11}$ s^{-1}, and hence is of the same order of magnitude as the experimentally found value of 1.2×10^{12} s^{-1}.[21]

In summary, the computed charge-transfer rates turn out to be large, so that the fastest hopping processes get to be close to the frequency scale characteristic of vibrational dephasing, a process that would induce a further charge delocalization. We also find that hopping processes which involve 2-fold and 3-fold coordinated sites are faster than the charge transfer within the dimer. In addition, the energy of these states is lower than that of the dead-end sites, so that their population is higher. Moreover, detrapping from a singly coordinated building block turns out to be the fastest process altogether. It turns out that the RHF studied here may allow fast charge transport over large distances along the backbone, given that the probability of exploring dead ends is low. This trend gets to be even more pronounced at low temperatures, where the charge-transfer rates obtained from eq 4.2. are $k_{32} = 7.1 \times 10^7$ s^{-1}, $k_{23} = 1.1 \times 10^{10}$ s^{-1}, $k_{31} = 3.6 \times 10^5$ s^{-1}, $k_{13} = 1.3 \times 10^{10}$ s^{-1}, and $k_{22} = 4.7 \times 10^8$ s^{-1} and the rate from $E_{A,11}$ is $k_{11} = 1.2 \times 10^7$ s^{-1}.

We stop to note that yet another experimentally observable quantity follows from the potential energy landscape displayed in Figure 6. We refer to the onset of the absorption spectrum in the infrared, which for a polaronic system is characterized by an intense charge-transfer band. For the RHF studied here, this onset lies at ~0.15 eV; we hence expect the low-energy tail of the absorption spectrum to exhibit a pronounced red shift with respect to the absorption of the molecule displayed in Figure 2.

5. Conclusions

In this work, we have studied the formation of polarons in regular hyperbranched polymers and their influence on the conduction properties of the latter. As topology, we have chosen regular hyperbranched fractals (RHFs). Unlike dendrimers, the RHFs obey scaling and are not limited in their size. Such systems can be constructed iteratively, and an outline for their synthesis has been recently suggested based on condensed triarlyamines.[20]

To describe the electronic structure, we have extended a π orbital tight-binding model by a nonretarded reaction field that takes the coupling of the system to a polarizable environment into account. The approach follows the concepts of Marcus' theory of outer-sphere charge-transfer reactions. The resulting Hamiltonian can be solved within the Hartree−Fock self-consistent-field approximation. For singly charged cations, the resulting charge distribution depends on the initial conditions. The symmetry of the molecule is broken by the interaction with the external field, and the positive charge may localize in the vicinity of each of the nitrogen atoms.

To address the question of charge transport, we have verified the applicability of a linear synchronous transit approach. Here, the density matrices of two adjacent basins of attraction of the SCF procedure have been interpolated, and the interpolation parameter serves as the reaction coordinate. We find that the depths of the traps depend on the coordination number of the corresponding monomers, and that the energy barriers for hopping range from 43.4 meV to 113.0 eV. At room temperature, this leads to hopping rates of the order of 10^{12} s^{-1}. At liquid nitrogen temperature, the computed spectrum of charge-transfer rates covers more than 4 orders of magnitude. We expect singly coordinated monomers to get rapidly depopulated, since they turn out to have a low trapping energy and to exhibit a small barrier with respect to charge transport. These monomers are mainly located at dead ends for the transport, so that these properties favor charge transport along the backbone. We therefore suggest to use hyperbranched triarylamines as bridging elements to enhance the mobility of holes in conducting polymers.

Acknowledgment. It is a pleasure to thank C. Lambert, T. Cramer, N. Utz, M. Rateitzak, C. von Ferber, C.A. Zell, P. Gräber, and A. Labahn for fruitful discussions and helpful comments. This work has been supported by the Deutsche Forschungsgemeinschaft. A.B. gratefully acknowledges support by the Fonds der Chemischen Industrie and the BMBF.

References and Notes

(1) Roovers, J. In *Star and Hyperbranched Polymers*; Mishra, M. K., Kobayashi, S., Eds.; Marcel Dekker: New York, 1999; p 285.
(2) La Ferla, R. *J. Chem. Phys.* **1997**, *106*, 688.
(3) Cai, C.; Chen, Z. Y. *Macromolecules* **1997**, *30*, 5104.
(4) Chen, Z. Y.; Cai, C. *Macromolecules* **1999**, *32*, 5423.
(5) Ganazzoli, F.; La Ferla, R.; Raffaini, G. *Macromolecules* **2001**, *34*, 4222.
(6) Biswas, P.; Kant, R.; Blumen, A. *Macromol. Theory Simul.* **2000**, *9*, 56.
(7) Biswas, P.; Kant, R.; Blumen, A. *J. Chem. Phys.* **2001**, *114*, 2430.
(8) Gurtovenko, A. A.; Gotlib, Yu. Ya.; Blumen, A. *Macromolecules* **2002**, *35*, 7481.
(9) Sunder, A.; Hanselmann, R.; Frey, H.; Mülhaupt, R. *Macromolecules* **1999**, *32*, 4240.
(10) Sunder, A.; Heinemann, J.; Frey, H. *Chem. Eur. J.* **2000**, *6*, 2499.
(11) von Ferber, C.; Blumen, A. *J. Chem. Phys.* **2002**, *116*, 8616.
(12) Vicsek, T. *Fractal Growth Phenomena;* World Scientific: Singapore, 1989.
(13) Jayanthi, C. S.; Wu, S. Y.; Cocks, J. *Phys. Rev. Lett.* **1992**, *69*, 1955.
(14) Jayanthi, C. S.; Wu, S. Y. *Phys. Rev. B* **1993**, *48*, 10188.
(15) Jayanthi, C. S.; Wu, S. Y. *Phys. Rev. B* **1993**, *48*, 10199.
(16) Jayanthi, C. S.; Wu, S. Y. *Phys. Rev. B* **1994**, *50*, 897.
(17) Schwalm, W. A.; Schwalm, M. K.; Giona, M. *Phys. Rev. E* **1997**, *55*, 6741.
(18) Blumen, A.; Jurjiu, A.; Koslowski, Th.; von Ferber, Ch. *Phys. Rev. E* **2003**, *67*, 061103.
(19) Jurjiu, A.; Koslowski, Th.; von Ferber, Ch.; Blumen, A. *Chem. Phys.* In press.
(20) Blumen, A.; von Ferber, Chr.; Jurjiu, A.; Koslowski, Th. *Macromolecules*, in press.
(21) Lambert, C.; Nöll, G. *J. Am. Chem. Soc.* **1999**, *121*, 8434. Lambert, C.; Gachler, W.; Schmälzlin, E.; Meerholz, K.; Bräuchle, C. *J. Chem. Soc., Perkin Trans.* **1999**, *2*, 577.
(22) Lambert, C.; Nöll, G. *Synth. Met.* **2003**, *139*, 57.
(23) Utz, N.; Koslowski, Th. *Chem. Phys.* **2002**, *282*, 389.
(24) Lambert, C.; Nöll, G.; Schelter, J. *Nat. Mater.* **2002**, *1* 69.
(25) May, V.; Kühn, O. *Charge and energy transfer dynamics in molecular systems*; Wiley-VCH: Berlin, Germany, 2000.
(26) Saraste, M. *Science* **1999**, *283*, 1488.
(27) Jortner, J.; Bixon, M., Eds. Electron Transfer−from isolated Molecules to Biomolecules Part One. *Adv. Chem. Phys.* **1999**, *106*. Jortner, J.; Bixon, M., Eds. Electron Transfer−from isolated Molecules to Biomolecules Part Two. *Adv. Chem. Phys.* **1999**, *107*.
(28) Demadis, D. K.; Hartshorn, C. M.; Meyer, T. J. *Chem. Rev.* **2001**, *101*, 2655.
(29) Moser, C. M.; Page, C. C.; Chen, X.; Dutton, P. L. *Subcell. Biochem.* **2000**, *35*, 1.

(30) Kuznetsov, A. M.; Ulstrup, J. *Electrochim. Acta* **2000**, *45*, 2339.
(31) Warshel, A. *Acc. Chem. Res.* **2002**, *35*, 385.
(32) Koslowski, Th. *J. Chem. Phys.* **2000**, *113*, 10703. Koslowski, Th. *Z. Phys. Chem. NF* **2001**, *215*, 1625. Koslowski, Th. *Phys. Chem. Chem. Phys.* **2003**, *5*, 2197.
(33) Lach, C.; Müller, P.; Frey, H.; Mülhaupt, R. *Macromol. Rapid Commun.* **1997**, *18*, 253.
(34) Möck, A.; Burgath, A.; Hanselmann, R.; Frey, H. *Macromolecules* **2001**, *34*, 7692. Möck, A.; Burgath, A.; Hanselmann, R.; Frey, H. *Polym. Mater. Sci. Eng.* **1999**, *80*, 173. Burgath, A.; Möck, A.; Hanselmann, R.; Frey, H. *Polym. Mater. Sci. Eng.* **1999**, *80*, 126.
(35) Casewit, C. J.; Colwell, K. S.; Rappé, A. K. *J. Am. Chem. Soc.* **1992**, *114*, 10035. Casewit, C. J.; Colwell, K. S.; Rappé, A. K. *J. Am. Chem. Soc.* **1992**, *114*, 10046.
(36) Harrison, W. A. *Electronic structure and the properties of solids*; Freeman: San Francisco, CA, 1980.
(37) Marcus, R. A. *J. Chem. Phys.* **1956**, *24*, 966. Marcus, R. A. *J. Chem. Phys.* **1956**, *24*, 979. Marcus, R. A. *Annu. Rev. Phys. Chem.* **1964**, *15*, 155.
(38) Georges, A.; Kotliar, G.; Krauth, W.; Rozenberg, M. J. *Rev. Mod. Phys.* **1996**, *68*, 13. Micnas, R.; Ranninger, J.; Robaskiewicz, S. *Rev. Mod. Phys.* **1990**, *62*, 113. Shen, S.-Q. *Int. J. Mod. Phys. B* **1998**, *12*, 709. Mancini, F.; Marinaro, M.; Matsumoto, H. *Int. J. Mod. Phys. B* **1996**, *10*, 1717.
(39) Rauhut, G.; Clark, T. *J. Am. Chem. Soc.* **1993**, *115*, 9127. Gröppel, M.; Roth, W.; Clark, T. *Adv. Mater.* **1995**, *7*, 927.
(40) Koslowski, Th. *J. Phys. Condens. Matter* **1997**, *9*, 613. Koslowski, Th. Koblischke, M.; Blumen, A. *Phys. Rev. B* **2002**, *66*, 064205.